Electronic Supplementary Information (ESI)

High-performance monoliths in heterogeneous catalysis with single-phase liquid flow

Christian P. Haas[a], Tibor Müllner[a], Richard Kohns[a,b], Dirk Enke[b], Ulrich Tallarek[a,*]

[a] Department of Chemistry, Philipps-Universität Marburg, Hans-Meerwein-Straße 4, 35032 Marburg, Germany

[b] Institute of Chemical Technology, Universität Leipzig, Linnéstraße 3, 04103 Leipzig, Germany

* Corresponding author. Tel.: +49-6421-28-25727; fax: +49-6421-28-27065.
E-mail address: tallarek@staff.uni-marburg.de (U. Tallarek).
URL: http://www.uni-marburg.de/fb15/ag-tallarek.

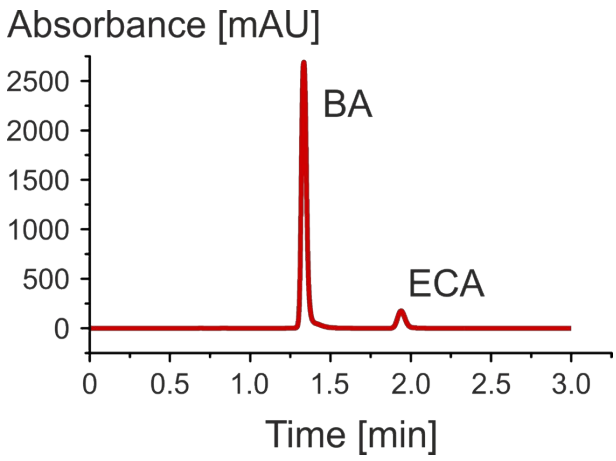

Fig. S1 Chromatogram (λ = 250 nm) of a solution containing 5 mmol L^{-1} benzaldehyde (BA) and 5 mmol L^{-1} ethyl *trans*-α-cyanocinnamate (ECC) in ethanol, recorded in the HPLC dimension under standard conditions.

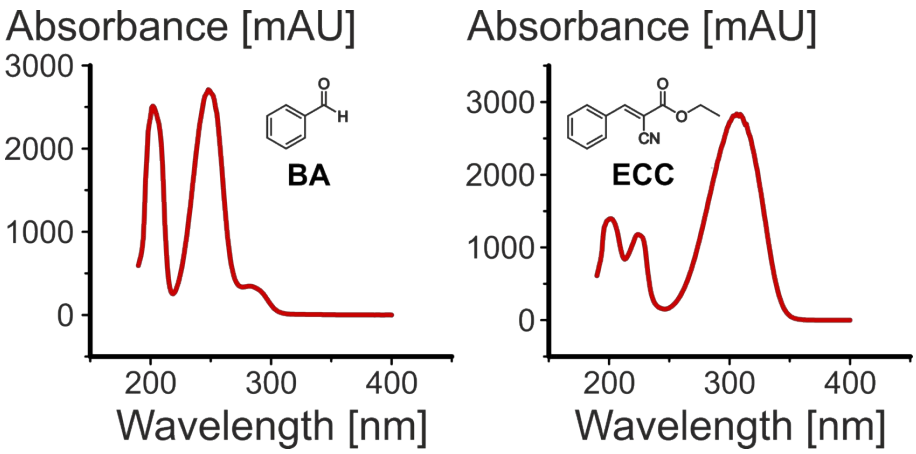

Fig. S2 UV/VIS absorption spectra of benzaldehyde (BA) and ethyl *trans*-α-cyanocinnamate (ECC) in 50:50 (v/v) water/ethanol.

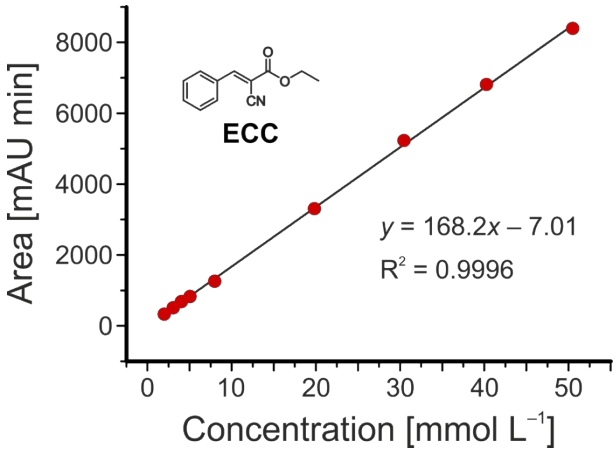

Fig. S3 Linear calibration graph for ethyl *trans*-α-cyanocinnamate (ECC) in 50:50 (v/v) water/ethanol for direct determination of ECC concentration in the HPLC dimension.

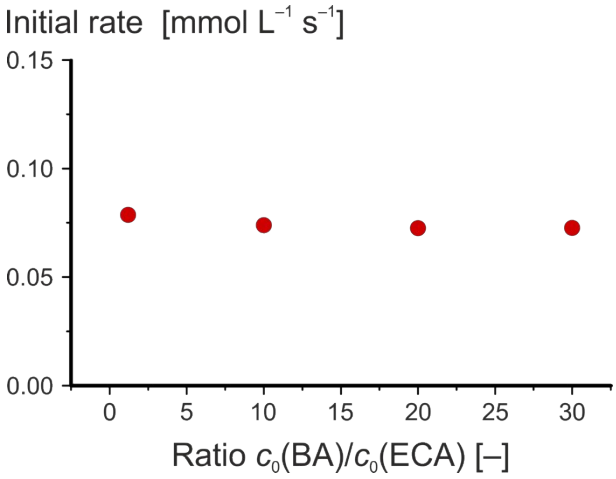

Fig. S4 Initial rate of the Knoevenagel condensation reaction between benzaldehyde (BA) and ethyl cyanoacetate (ECA). The initial concentration of ECA was constant at c_0(ECA) = 5 mmol L^{-1}, while the initial BA concentration was increased up to c_0(BA) = 150 mmol L^{-1} at a temperature of T = 25 °C and in ethanol as solvent.

Isothermal microreactor operation

The microreactor was assumed to remain under isothermal conditions, since reactant solutions with low concentrations were used. To validate this assumption, the amount of released reaction heat was calculated for different temperatures and flow rates, treating the microreactor as an ideal adiabatic plug-flow reactor operating in the steady state. In reality, heat exchange between the microreactor and its environment (thermostatted air) occurs, but this will be very poor due to the low heat-transfer coefficients of silica and the PEEK cladding of the monolith. However, even under adiabatic conditions the released reaction heat results in small temperature changes of the reaction medium as shown below. The temperature change ΔT between the adjusted and controlled temperature at the inlet (T_{start}) and the outlet (T_{end}) of the microreactor was calculated according to:

$$\Delta T = T_{start} - T_{end} = \Delta H \; c(ECC) \frac{M(EtOH)}{c_p(EtOH) \; \rho(EtOH)} \tag{S1}$$

Here, ΔH is the reaction enthalpy, which is given in the literature for very similar Knoevenagel reactions as $\Delta H \sim 30$ kJ mol^{-1}.[1] Combined with c(ECC) as product concentration in the reaction solution, the heat released on the microreactor can be estimated.

The heat capacity of the fluid was approximated as that for pure ethanol using the molar heat capacity c_p(EtOH) ~ 112 J mol^{-1} K^{-1}, the molar mass M(EtOH) = 46.07 g mol^{-1}, and the density ρ(EtOH) = 0.785 g cm^{-3}.[2] All values were taken for a temperature of 298.15 K and assumed as constant over this moderate temperature range, since an estimate of the temperature changes is sufficient. Selected values of ΔT are summarized in Table S1. From these data, it becomes clear that the temperature changes are very small and insignificant, since the thermostatted column compartment itself shows only a specified temperature accuracy of ±0.8 °C (*cf.* Section 2.4 in the main text). Consequently, isothermal operation of the microreactor can be assumed.

Turnover frequency

Turnover frequency (TOF) of the catalytically active centers was calculated in the form of mean TOFs over the entire reactor as follows:

$$TOF = \frac{Q\ c(ECC)}{n_{cat}} \tag{S2}$$

Here, Q is the volumetric flow rate, c(ECC) is the product concentration in the reaction solution, and n_{cat} is the amount of catalytically active (and available) groups on the silica surface of the microreactor (0.343 mmol, *cf.* Sections 2.3 and 3.3 in the main text). The TOFs for selected temperatures and flow rates are summarized in Table S1.

Table S1. Temperature changes on the microreactor ΔT assuming adiabatic plug-flow operation in the steady state, resulting temperatures at the outlet T_{end}, and the corresponding turnover frequencies (TOFs) for different adjusted temperatures T_{start} and flow rates Q.

T_{start} [K]	Q [mL min^{-1}]	ΔT [K]	T_{end} [K]	TOF [h^{-1}]
283.15	0.5	–0.15	283.30	4.92
283.15	3.0	–0.50	283.65	2.73
293.15	0.5	–0.24	293.39	7.87
293.15	3.0	–0.65	293.80	3.55
298.15	0.5	–0.30	298.45	9.84
298.15	3.0	–0.71	298.86	3.87
303.15	0.5	–0.40	303.55	13.09
303.15	3.0	–0.77	303.92	4.19
313.15	0.5	–0.50	313.65	16.28
313.15	3.0	–0.79	313.94	4.31

Calculation of the Thiele modulus

The Thiele modulus accounts for the competition between the Knoevenagel reaction at the APS surface (represented by k_2) and the limitation of transport of the reactant ECA by diffusion in the mesoporous skeleton of the monolith (represented by D_{eff}):

$$\Phi = L_{skel}\sqrt{\frac{k_2}{D_{eff}}} = \frac{V_{skel}}{A_{ext}}\sqrt{\frac{k_2}{D_{eff}}} \tag{S3}$$

The characteristic diffusion length L is generally defined as the volume-to-surface ratio of the spatial domain, in which diffusion-limited transport takes place. In this study, L_{skel} in Eq. S3 refers to purely diffusive transport in the mesopores of the silica skeleton (*cf.* Fig. 3B in the main text). For determination of L_{skel} we used physical reconstructions of the silica monoliths[3] obtained by confocal laser scanning microscopy to extract the total volume and external surface area of the skeleton (white phase in Fig. 9). On that image-based analysis we receive:

$$L_{skel} = \frac{V_{skel}}{A_{ext}} = 0.22\ \mu m \tag{S4}$$

Further, the value of D_{eff} for ECA (Eq. S3) in the rate-determining step of the reaction (Scheme 2) was estimated by its molecular diffusion coefficient D_{m} in bulk solution and from the porosity and tortuosity of the mesoprous skeleton according to:

$$D_{eff} = D_m\frac{\varepsilon_{meso}}{\tau_{meso}} \tag{S5}$$

While the intraskeleton porosity $\varepsilon_{\text{meso}} = 0.68$ and tortuosity $\tau_{\text{meso}} = 1.25$ for the employed silica monoliths have already been summarized in Table 1 (main text),[4] the value of D_{m} was estimated using the Wilke–Chang equation[5] applied to ECA in pure ethanol. The Wilke–Chang equation describes the molecular diffusion coefficient D_{AB} for the solute ECA (subscript A) in the solvent ethanol (subscript B) as:

$$D_{AB} = 7.4\cdot10^{-8}\frac{(\varphi_B M_B)^{0.5}\,T}{V_{b,A}^{0.6}\,\mu_B} \tag{S6}$$

For the solvent, φ_B is the association factor, M_B the molar mass, and μ_B the dynamic viscosity, whose temperature-dependence can be approximated as:[6]

$$\mu_B(T) = \exp\left(-6.21 + \frac{1614}{T} + 0.00618\,T - 1.132\cdot10^{-5}\,T^2\right) \quad \text{(S7)}$$

The molar volume at the normal boiling point $V_{b,A}$ can be derived using the critical volume $V_{c,A}$, critical temperature $T_{c,A}$, boiling point $T_{b,A}$, and acentric factor ω_A of the solute ECA:[7]

$$V_{b,A} = 7.047345 + 0.4\,V_{c,A} + \left(0.01724 + \frac{15.3765}{T_{c,A}} + 0.004387\,\omega_A\right)T_{b,A} \quad \text{(S8)}$$

All required thermophysical data for ECA can be found in the literature and are summarized in Table S2,[8] together with the resulting molar volume at the normal boiling point.

Table S2. Thermophysical properties of ethyl cyanoacetate (ECA).[8]

$V_{c,A}$ [mL mol^{-1}]	$T_{c,A}$ [K]	$T_{b,A}$ [K]	ω_A [–]	$V_{b,A}$ [mL mol^{-1}]
358.00	679.00	482.20	0.426	170.38

Returning to the Wilke-Chang equation, the ECA diffusion coefficient at different temperatures was estimated using the association factor of $\varphi_B = 1.5$ and a molar mass of $M_B = 46.07$ g mol^{-1} for the solvent ethanol. Experimental values for the reaction rate constant k_2 were determined in the temperature range of T = 10–40 °C in steps of 5 °C. All temperature dependent values including the targeted Thiele moduli are summarized in Table S3.

Table S3. Viscosity of ethanol, molecular and effective diffusion coefficients of ECA, as well as the rate constants of the rate-determining step in the Knoevenagel condensation, and the resulting Thiele moduli in the temperature range of 10–40 °C.

T [K]	μ_B [cPa]	D_{AB} [m^2 s^{-1}]	D_{eff} [m^2 s^{-1}]	k_2 [s^{-1}]	Φ [–]
283.15	1.39	5.72×10^{-10}	3.11×10^{-10}	1.00×10^{-2}	0.00125
288.15	1.26	6.44×10^{-10}	3.50×10^{-10}	1.21×10^{-2}	0.00129
293.15	1.14	7.22×10^{-10}	3.93×10^{-10}	1.51×10^{-2}	0.00136
298.15	1.04	8.08×10^{-10}	4.39×10^{-10}	1.88×10^{-2}	0.00144
303.15	0.95	9.01×10^{-10}	4.90×10^{-10}	2.30×10^{-2}	0.00151
308.15	0.87	1.00×10^{-9}	5.45×10^{-10}	2.81×10^{-2}	0.00158

313.15	0.79	1.11×10^{-9}	6.05×10^{-10}	3.40×10^{-2}	0.00165

128

References

1 W. H. Correa, J. K. Edwards, A. McCluskey, I. McKinnon, J. L. Scott, *Green Chem.*, 2003, **5**, 30–33.

2 NIST WebBook, http://webbook.nist.gov/chemistry/ (accessed April 2017).

3 D. Hlushkou, K. Hormann, A. Höltzel, S. Khirevich, A. Seidel-Morgenstern and U. Tallarek, *J. Chromatogr. A*, 2013, **1303**, 28–38.

4 K. Hormann and U. Tallarek, *J. Chromatogr. A*, 2014, **1365**, 94–105.

5 C. R. Wilke and P. Chang, *AIChE J.*, 1955, **1**, 264–270.

6 CHERIC, http://www.cheric.org/research/kdb/hcprop/cmpsrch.php (accessed March 2017).

7 I. E. Maloka, *Pet. Sci. Technol.*, 2005, **23**, 133–136.

8 C. L. Yaws, *Thermophysical Properties of Chemicals and Hydrocarbons*, William Andrew, Norwich, NY, 2014.